TECHNICAL UNIVERSITY OF CLUJ-NAPOCA

ACTA TECHNICA NAPOCENSIS

Series: Applied Mathematics, Mechanics, and Engineering
Vol. 64, Issue III, September, 2021

CONSIDERATIONS ON ORDER ANALYSIS OF A ROTATING MACHINERY TEST RIG

Iulian LUPEA

Abstract: *Order analysis is used to observe the vibration of machine elements of a rotating machinery test rig. The rotational speed of the dc motor integrated with the gear reducer and subsequent shafts, changes over time during run-ups and coast-downs. Orders viewed as harmonics of the tracked shaft rotational speed are employed to certify estimated motor stator poles and armature windings, gear pair ratios on the reducer gearbox and to sustain vibro-acoustic diagnosis of the machine elements of the test rig. This is a prerequisite to the application of some methods to detect faulty machine elements of the test rig, starting from time varying rotational speed measurements.*
Keywords: *Order analysis, condition monitoring, machine element fault.*

1. INTRODUCTION

As a machine element (shaft, gear, belt etc.) rotates it generates vibrations expressing specific behaviors coming from normal functioning or from machine element faults. When the speed of rotation changes, like in wind turbines planetary gearbox, car transmission units, the vibration amplitude and the frequency generated by the component changes in relation to the RPM of a reference machine element like a rotating shaft. With the equal time sample mode of the acquired signal when the rotating speed changes, smearing of the discrete frequencies in the frequency domain takes place. Frequency lines of the spectrum often are indicating machine element faults; after the frequency smearing, frequency lines no longer are trusty indicators of the defects. For rotating and reciprocating machines the analysis of vibration signals is often preferred in terms of order spectrum rather than the frequency spectrum. The equal angle interval resampling (angular resampling) of the acquired signal can convert the nonstationary signal in time domain into stationary signal in angle domain by using order tracking technique [2], [23]. Faults on gears, belts or bearings alter the normal functioning conditions of the mechanical transmission causing higher level of vibration as well as a decrease in the transmission quality or the machine breakdown. On one side, errors are coming from the manufacturing, mounting or installation errors, etc. On the other side, errors can be generated from the operation of the gears. Some faults are affecting all the teeth sides causing wear of the gear while other faults are localized like cracks, spalling and pitting. Vibrations are coming from normal functioning of the gear as well, from meshing forces or the repetitive shocks when the mating teeth are engaging and coming into contact.

Order analysis is applied intensively to machine condition monitoring and NVH testing [1] on mechanical systems with rotating and reciprocating components. Orders with amplitude and phase can be perceived as harmonics of the tracked rotational frequency. Order tracking technique is an important approach for fault diagnosis in rotating machinery [15], [16], [19].

Some electrical frequencies on permanent magnet DC motors are coming from the DC drive which gets the power from an AC power source. The motor drive cuts off the negative

Received: 29.07.21; **Similarities**: 14.09.21: **Reviewed**: 20.08/31.08.21: **Accepted**:15.09.21.

portion of the sine wave in order to get a constant "+" voltage. This is done with a silicon controlled rectifier (SCR) for large power dc motors (which is not the case in the test rig under observation here). The orders depends on whether the drive is full-wave rectified or half-wave rectified and the line frequency (50 Hz). Frequency line harmonics like 2x, 3x, 4x, 5x and SCR firing frequency (FSCR) for full wave rectified or 2x, 3x and FSCR for half wave rectified may be seen. Sidebands around FSCR can be present as well, with proper interpretation [3], [10].

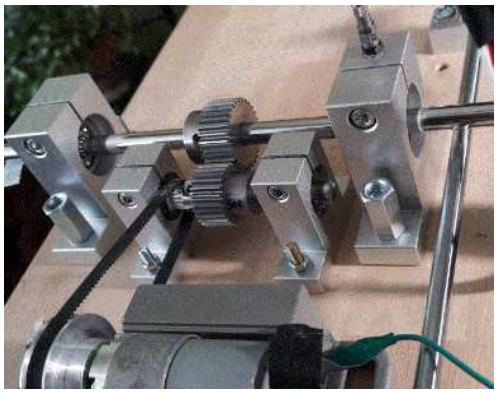

Fig. 1. Test rig: DC motor, reducer, timing belt, ball bearings and a gear pair

In the paper the orders analysis is performed on a transmission chain, observing orders extracted from vibration signals and associated to vibration patterns generated from normal and abnormal machine elements behavior and the dc gear motor. The reducer gear pairs are observed along with the timing belt that transfer the rotation to a distal and larger gear pair (module 1mm, Z1=26, Z2=31) sustained on two shafts placed on ball bearings. The measurements are performed by using an accelerometer and a tachometer. The signals were acquired on two analog channels out of four channels of a NI USB 4431 acquisition board. The orders on color maps are obtained with Labview applications. Vibration patterns and orders of the machine elements are identified and discussed in relation to possible part faults or defects. Comments on the condition monitoring of the device are formulated. Order tracking for the time varying speed machines may be employed for the parameter extraction for classical machine learning techniques, artificial neural networks and deep learning neural network architectures for the faults identification and classification [12], [13], [17].

2. THE ROTATING MACHINERY AND ACQUISITION SYSTEM SET-UP

The device under observation involves some common machine elements like helical and spur gear pairs of the reducer, a timing belt, another spur gear on parallel shafts on ball bearings (Fig. 1). The observed transmission chain is animated by a brushed Pololu DC motor (12 Volts), coupled with the reducer of three stages (Fig. 2).

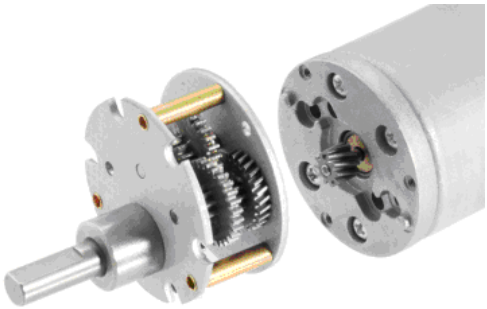

Fig. 2. Gearmotor with Helical Pinion and the gearbox removed [24]

The metal gearbox reducer is characterized by the 18.75:1 ratio. The first stage of the reducer is a helical gear pair for reduced noise

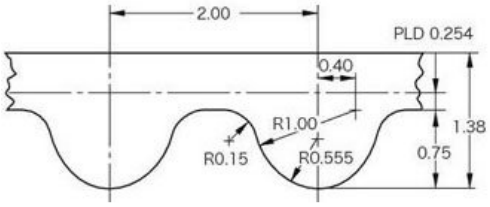

Fig. 3. Timing belt teeth profile [25]

and vibrations and improved efficiency [24] followed by two stages of spur gears. The reducer's output shaft is of 6 mm diameter, D-shaped. The motor speed controller input voltage range is 9V to 60V and the output current range from 0 to 20A. The rotation from the motor reducer output shaft is transferred to a gear pair through a timing synchronous belt (2mm tooth pitch, 6mm wide), having a special profile with rounded teeth which reduces

backlash (Figure 3). This belt type is often used for precision 3D printers and CNC machines. It is a Neoprene (oil-resistant substitute for natural rubber) - synthetic rubber reinforced with fiberglass cords for superior strength [25]. A timing Belt aluminum pulley of 60 teeth is mounted on the 6 mm diameter gearbox output shaft. This is the driver sheave of the timing belt.

A NI USB-4431 acquisition, 24bit, 102.4 kS/s dynamic acquisition board is used with the first two analog channels (out of four simultaneous acquisition channels).

The tachometer laser beam is pointing on the side of the driver pulley. A uniaxial IEPE piezoelectric accelerometer (101mV/g) is glued vertically on the reducer gearbox top.

The load on the out shaft is obtained by friction imposed on the shaft by a tensioned plastic ribbon wrapped around the shaft and in contact with the shaft for more than π radians.

3. ODER ANALYSIS FOR THE GEARBOX REDUCER WITH LABVIEW

The reducer three gear pairs (p1, p2, p3) are schematized in Figure 4.

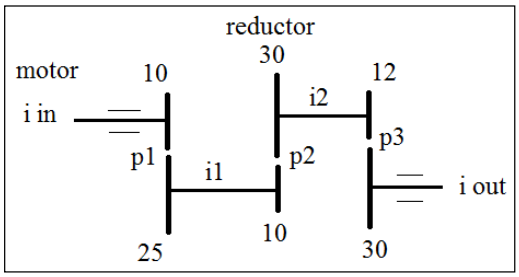

Fig. 4. Reducer kinematic chain

The relation between the input and output turning speed is as following (1):

$$i_{in} \cdot \frac{10}{25} \cdot \frac{10}{30} \cdot \frac{12}{30} = i_{out} \text{ or:} \quad (1)$$

$$i_{in} = i_{out} \cdot \frac{30}{12} \cdot \frac{30}{10} \cdot \frac{25}{10} \quad (2)$$

A log data application is run with acquisition on two channels, one analog channel for the accelerometer mounted vertically on top of the reducer housing and the second analog channel for the tachometer voltage pulses acquisition (one pulse per shaft revolution). The sampling rate is 4kHz resulting the frequency bandwidth of 2kHz. On the Labview acquisition application the sampling per channel input being 2000 (sampling) results two readings per second or twice per second the DAQmx Read.vi function is run and the data saved in a log file. DAQmx Read.vi returns a 1D array of waveforms (dt=0.00025seconds). Each element of the array is a waveform corresponding to an input channel. The typical acquired waveform from the accelerometer is depicted in Figure 5. In the same figure the speed (RPM - revolutions per minute) versus time profile can be seen, observing a run-up portion followed by a run-down. The recording time is 60 seconds of continuous acquisition simultaneous on the

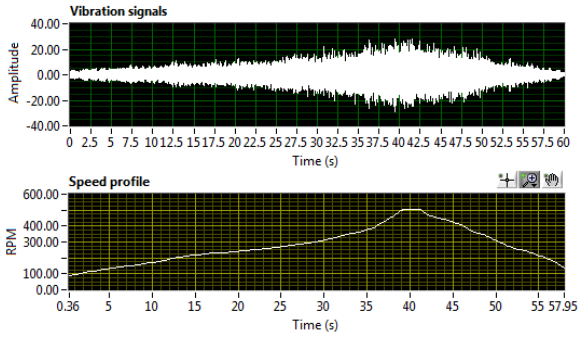

Fig. 5. Acquired vibration waveform and the output shaft speed profile

two channels. A second application is loading the logged data and the Order Analysis, after the resampling, is performed offline. The colormap diagram (intensity graph) as a first step in order analysis with frequency versus time (30 seconds) is shown in Figure 6. The maximal level of vibration acceleration is 70dB for a reference dB of 1*10^-6 [m/s^2] in order to have the lowest orders visible.

The overview information regarding the principal order lines and the frequency interval with strongest vibration can be observed on this spectral map. This colormap shows the vibration spectrum amplitude increasingly from blue to red in function of the frequency or the orders. The vibration amplitude can be observed in function of the rotational speed or the time. The analysis observed the conversion of the original even time spaced signal to even angle signal.

3.1. Spindle rotation speed orders:

The first order (1X) is associated to the revolution speed of the reducer output shaft.

The 2.5X order (not observed in the color map, Figure 6) is associated to the i2 shaft rotational speed:

$$i2=Iout\cdot\frac{30}{12} \quad (3)$$

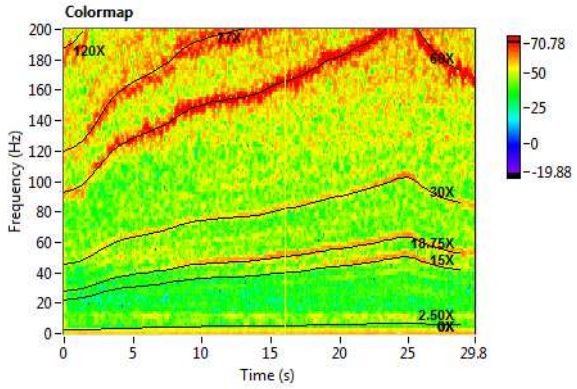

Fig. 6. Reducer gear pairs low orders acc. on gearbox, tacho on 60teets wheel

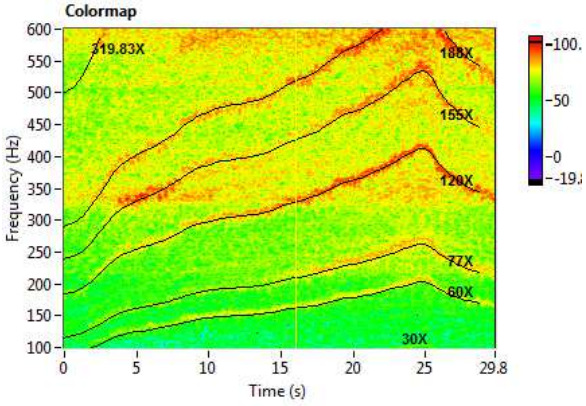

Fig. 7. Colormap: the accelerometer on the gearbox and tacho on the 60teeth belt wheel

The 7.5X order (light trace in color map) is associated to the i1 shaft rotational speed:

$$i1=i2\cdot\frac{30}{10}=Iout\cdot 2.5\cdot 3 \quad (4)$$

The 18.75X order (bold trace in color map) is associated to the Iin rotational speed or the output shaft of the DC motor:

$$Iin=i1\cdot\frac{25}{10}=Iout\cdot 7.5\cdot 2.5 \quad (5)$$

The engagement between the timing belt and the pulley with 60 teeth is associated to the 60X order which is pronounced in the color map.

$$Obelt1=Iout\cdot \mathbf{60} \quad (6)$$

3.2. Gear mesh frequencies (GMFs)

$GMF_{12/30}$ of gear pair Z12, Z30 is observed along order 30th:

$$GMF_{12/30}=Iout\cdot 30 \quad (7)$$

GMF of gear pair Z30, Z10 is observed along order 75th (bold trace in color map):

$$GMF_{10/30}=i2*30=Iout\cdot 2.5*30 \quad (8)$$

GMF of gear pair Z10, Z25 is observed along order 187.5th (bold trace):

$$GMF_{10/25}=Iin*10=Iout*18.75*10 \quad (9)$$

Other harmonics like 7th, 8th and 9th of the Iout are observable.

3.3. Orders associated to the DC motor

This Pololu dc motor has permanent magnet stator with two poles and armatures with three coils. Considering the speed of the reducer output which is tracked by the tachometer:

$$PolRot=3\cdot Iout\cdot 18.75=Iout\cdot 56.25 \quad (10)$$

Order 56.25X is well observed. The second harmonics 112.5X of the coils rotational speed is observed as well.

Orders associated to DC Power, cogging torque and magnetic field are present for some large motors. The electromagnetic vibration of the motor is mainly caused by electromagnetic exciting force which causes deformation of the mechanical structure and excites the motor to vibrate. Radial pulsating forces and bending moments on poles are interacting between the stator and the rotor resulting elastic deformation and vibration [3].

The DC motor torque ripple is caused by factors like cogging torque, the interaction between the MMF and the air gap flux harmonics or mechanical imbalance. An increased number of poles can reduce the level of torque ripple.

The cogging torque is due to the magnetic attraction between rotor and stator when the sides of the rotor teeth line up with the sides of the stator teeth (rotor/stator alignment), hence preventing the smooth rotor rotation [10]. The motor requires torque to overcome that attraction. An increased number of poles and twisted-slot reduce cogging poles or having an encoder by using electronic drive techniques. The torque ripple and cogging torque cause vibrations and noise. To diminish these effects a 12V motorcycle battery has been used alternatively to power the electrical motor.

3.4. Structural resonances

At about 340 Hz, 680 Hz and 900 Hz horizontal lines on the spectrum versus time are observable in Figure 8, indicating some

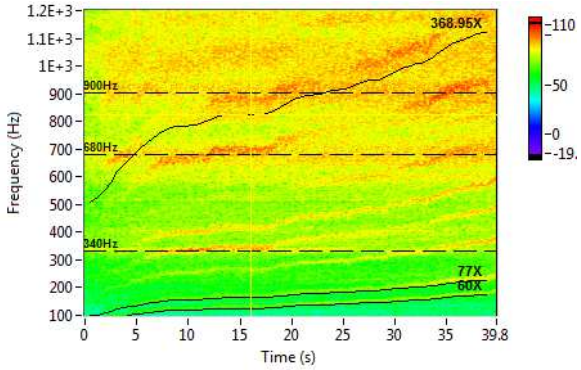

Fig. 8. Structural resonances

structural resonances of the test rig. These are not sensitive to the rotational speed.

3.5. Order power spectrum

Based on FFT, the order power spectrum is derived which is showing the power spectrum for all orders in the specified time interval.

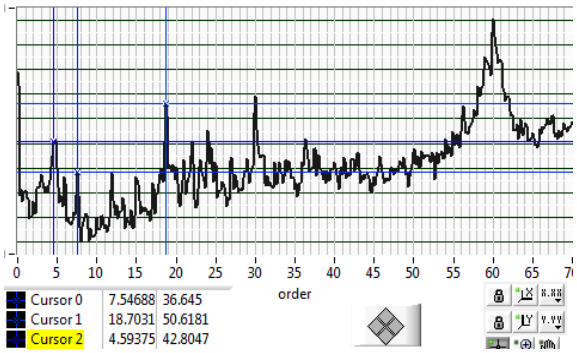

Fig. 9. Order power spectrum

Dominant order magnitude and phase can be observed and dominant and individual order waveforms can be extracted. Gabor transform and expansion is used for time waveform extraction [23]. Order 7.5X (Figure 9) is associated to the i1 shaft rotational speed and Iin (order 18.7X) rotational speed or the output shaft of the DC motor.

4. ODER ANALYSIS FOR THE GEAR PAIR ON BALL BEARING SHAFTS

4.1. Orders for tacho pointing on 8mm shaft and accelerometer on 8mm shaft support

The tachometer laser beam is pointing to the reflecting label of the pinion (26 teeth) shaft (Figure 1). The accelerometer is moved on the 8mm shaft support. On the colormap (Figures 10, 11) the 26th order or the 1xGMF is well observed. The 2xGMF (52th order) is pronounced. 3xGMF is less pronounced and both the 4xGMF (order 104X) and 5xGMF (order 130X) are very pronounced. At the intersection of the 52th order with the 335Hz spectrum line the high vibration amplitude is visible, assuming that a natural mode of vibration of the structure is excited.

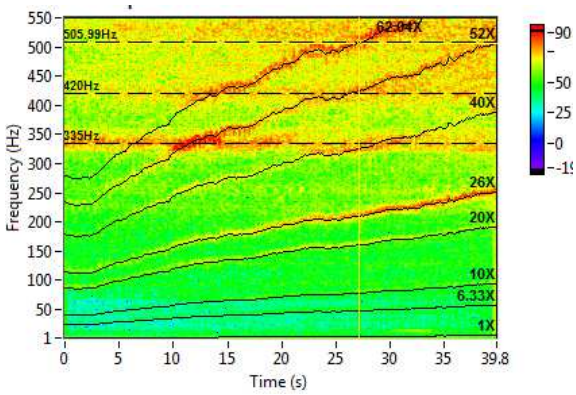

Fig. 10. Accelerometer on the 8mm shaft support and tacho on the 8mm shaft end

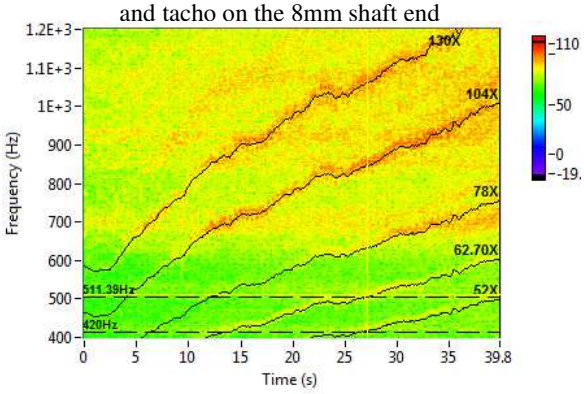

Fig. 11. Higher harmonics of the GMF, acc. on 8mm shaft support and tacho on the 8mm shaft

The 20th and 40th orders coming from the meshing between the aluminum sheave (20 teeth and mounted on the 8mm shaft) and the belt can be clearly seen (Figure 10) but less bold then the GMF orders.

In case the tooth load is increased by enforcing the load at the second shaft, the 1xGMF is more pronounced. A high peak in spectrum for the GMF, specially when an increase in sidebands and harmonics is not present, indicates that tooth load has increased; this aspect often does not indicate a defect.

The fundamental belt pass frequency (11):

$$F_{bp} = \pi D_2 / L \cdot f_2 = \pi D_1 / L \cdot f_1 \qquad (11)$$

is very low, where D_1, D_2 are the pitch diameter of the driver and respectively the driven pulley, L the belt length and f_1, f_2 are the rotational speed (Hz) of the driver and respectively the driven sheaves. For lose (or worn) belt the 2X F_{bp} and 3X F_{bp} orders are more pronounced. Higher peak (comparing to the F_{bp}) in frequency spectrum, at 1X f_1 or 1X f_2 shows up for pulley alignment problems. The resonance of the belt can cause spectrum higher peaks when the belt's natural frequency coincides with the driving or the driven pulley rotational frequency.

4.2. Orders for tacho pointing on 10mm shaft

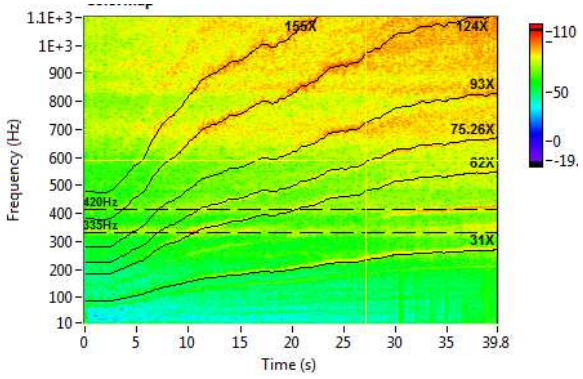

Fig. 12. Accelerometer on the 8mm shaft support and tacho on the 10mm shaft end

When tachometer beam is pointing to the reflected label placed on the 10mm diameter shaft the same 1xGMF is observed at the 31st order (Figure 12) and the bold and visible harmonics 2xGMF (62X order), 3xGMF (93X order), 4xGMF (124X order) and 5xGMF (155X order). The shaft rotational speed is lower (comparing to the 8mm shaft) and the orders are higher resulting the same GMF (the pinion on the 8mm shaft has 26 teeth and the gear on the 10mm shaft has 31 teeth).

The gear mesh frequency of the gear pair (gear module of 1mm) is:

$$GMF = n1 \cdot 26 = n2 \cdot 31 \qquad (12)$$

The rotational speed (n1) of the 8mm input (pinion) shaft when the 10mm shaft rotational speed is known (tacho), is:

$$n1 = n2 \cdot 31/26 \qquad (13)$$

In the colormap (Fig. 13) the order number 23.85 belongs to the timing belt meshing with the driven (20 teeth) aluminum pulley mounted on the 8mm shaft (14). The tachometer is pointing on the large (10mm) shaft (n2):

$$order = n2 \cdot 1.19 \cdot 20 \qquad (14)$$

The 23.85th order, the second harmonic at 47.6 X and the first subharmonic at 11.93 X can be seen in the colormap depicted in Figure 13.

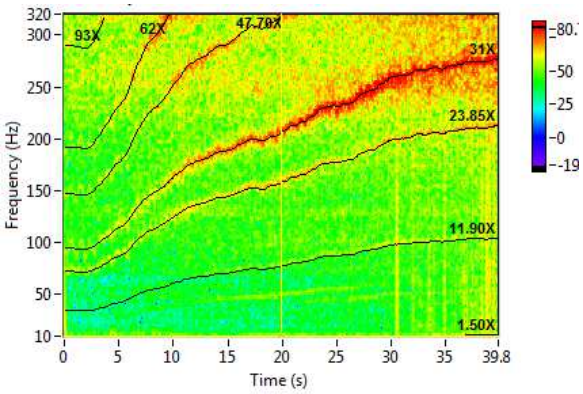

Fig. 13. Belt meshing with 20 teeth sheave, tacho on 10mm shaft and acc. on 8mm shaft

4.3. Gear pair backlash and misaligned gears

Gear pair backlash often results when the pinion or the gear is eccentric. For this case we will see an increase in amplitude of the 1X shaft rotational speed sidebands around the GMF peak. The sidebands will correspond to the speed of the pinion shaft or the gear shaft that is eccentric. When unloaded backlash causes an increased vibration at GMF.

The impacting resulting from the gear mesh may excite some natural frequencies of the gears. When a frequency peak rises, with a broad base, with 1X sidebands, it is likely to be the natural frequency of the gear.

Misalignment (angular or parallel) of coupled adjacent shafts often causes a high 1X or 2X respectively shaft turning speed

vibration. When gears are misaligned we shall see the 1xGMF peak increased in amplitude, but the second gearmesh harmonic (2xGMF) peak will increase far more. While 1X turning speed sidebands will be present, 2X sidebands will be stronger. The 3xGMF peak and its sidebands will also increase in amplitude, therefore it is important to set the Fmax of the FFT analysis larger than three times the gearmesh frequency.

The measured angle between gear axles in horizontal plane (Figure 14) is $a\tan((7.45-7.1)/72)$ resulting an angle α of 0.278 degree. As a countermeasure one bearing support is translated in order to decrease the angle between the two shafts (supporting spur gears) to α=0.048.

Fig. 14. Measuring distance between shafts

The second GMF harmonic order is not to much affected excepting for some high vibration level caused by resting longer time in the frequency band with structural resonance in the time period from 9th to 14th second of the test. The 3xGMF (93rd order) is clearly not so pronounced like in the previous test with α=0.278. Hence, the misaligned gears are coming with increased vibration level even in the higher GMF harmonics.

5. CONCLUSIONS

Fault diagnosis of machine elements is a pattern recognition problem of the vibration signal from which fault features has to be extracted. A test rig has been built to observe orders of various machine elements like gear pairs on the reducer, a timing belt, a gear pair on shafts on rolling bearing and to predict machine elements faults. A tachometer and an accelerometer are used to monitor the shafts rotational speed and the vibration acceleration on the reducer housing and the rolling bearing supports. A NI USB acquisition system and proper Labview applications are used to acquire and process acquired data. Order analysis is performed and the orders are assessed on colormaps being associated to the test rig machine elements. Some orders are associated to the normal functioning of the parts and others are coming from machine elements faults. Order power spectrum was used to assess the power on orders and to detect the contribution of the orders to the overall vibration level. Orders of the test rig with faulty parts (after the replacement of the parts without faults) is under study, in parallel with the spectra at constant rotational speed. Artificial intelligence machine learning-based fault diagnosis methods announced good performances in health monitoring of rotating machinery parts. Colormaps from run-up and cost-down and from order tracking will be used to feature extraction for machine learning techniques.

6. REFERENCES

[1] Arthur R. C., The Simplified Handbook of Vibration Analysis, 1992.

[2] Fyfe,K.,R., Munck,E., *Analysis of computed order tracking*, Mechanical Systems and Signal Processing, 11(2), 1997.

[3] Hong, J., et all., *PM Pole With Axial Varied Width for Vibration Mitigation in PM Brush DC Motors*, IEEE Transactions on industrial electronics, vol. 66, no. 5, may 2019.

[4] Lupea, I., *Sound absorption coefficient measurement set-up by using Labview and a simple impedance tube*, Acta Technica Napocensis, Series: Applied Mathematics, Mechanics, and Engineering, Vol. 62, Issue IV, November, 2019.

[5] Lupea, I., Vibration and noise measurement by using Labview programming, 2008.

[6] Luo.J., Hang,Z., Zhong,M., Lin,Z., *Order Spectrum Analysis for Bearing Fault Detection via Joint Application of Synchrosqueezing Transform and Multiscale Chirplet Path Pursuit*, Hindawi Publishing Corporation, Shock and Vibration, 2016.

[7] Maurice L. Adams, Jr., Rotating Machinery Vibration, CRC Press, 2000.

[8] Mogal, S.P., Lalwani, D.I., *Experimental investigation of unbalance and misalignment in rotor bearing system using order analysis*, Journal of Measurements in Engineering, Vol. 3, Issue 4, 2015.
[9] Norton, M P., Karczub, D G. Fundamentals of noise and vibration analysis for engineers (z-lib.org)], 2003
[10] Patel,A., Kapil, A., *Analysis of Cogging Torque Reduction by Increasing Stator Slot Depth in Brushless DC Motor,* 2nd Int. Conf. on Multidisc. Research & Practice
[11] Randall, R.,B., Vibration-based Condition Monitoring: Industrial, Automotive and Aerospace Applications, 2011.
[12] Rodrigues,C.E., e.a., Machine Learning Techniques for Fault Diagnosis of rotating machines using spectrum images of vibration orbits, doi: 10.48011/asba.v2i1.110 www.sba.org.br/ open_journal_systems/
[13] Scheffer C., Girdhar P., Practical Machinery Vibration Analysis and Predictive Maintenance, First Edition, Newnes, 2004
[14] Taylor, J., The vibration analysis handbook, 2019.
[15] Wang, KS, Feng,K., Zuo,M., *An order spectrum based method to ensure consistent monitoring through Vold-Kalman filter order tracking*, 19th World Conf. Non- Destructive Testing, 2016
[16] Wu,J-D, Wang, Y., Chiang,P., Bai,M., *A study of fault diagnosis in a scooter using adaptive order tracking technique and neural network*, Expert Systems with Applications, 36 (2009) 49–56.
[17] Zhao,D., Li,J., Cheng,W, *Feature Extraction of Faulty Rolling Element Bearing under Variable Rotational Speed and Gear Interferences Conditions*, Hindawi Publishing Corporation Shock and Vibration, Vol. 2015
[18] **www.bksv.com/media/doc/bv0052.pdf, Brüel and Kjær, Technical review: Characteristics of the Vold-Kalman Order Tracking Filter, 1999.
[19] **www.dewesoft.com, Order Tracking Measurement and Analysis, 2021
[20]**www.mathworks.com/matlabcentral/ fileexchange/32639-vold-kalman-order-tracking-code
[21] ** www.mobiusinstitute.com
[22] ** ni.com, Labview, National Instruments Sound and vibration measurement suite, 2018.
[23] ** ni.com.; Manuals, Getting Started with Order Analysis, and Order Analysis Toolkit User Manual, 2007
[24] ** www.pololu.com
[25] ** https://robu.in/product/2- meter- x-gt2- open- timing-belt-6mm-width/
[26] ** www.skf.com

Consideraţii asupra ordinelor generate de vibraţiile unui stand cu componente în rotaţie

Rezumat*:* In articol sunt măsurate ordinele generate de vibraţiile componentelor unui stand acţionat de un motor de curent continuu cu reductor în trei trepte. Sistemul de achiziţie foloseşte două canale ale unei plăci de achiziţie cu eşantionare simultană şi măsurare de la un accelerometru şi un tahometru; turaţia este variabilă. De la motoreductor mişcarea este transmisă prin curea dinţată spre o pereche de roţi dinţate susţinută de arbori şi lagăre cu rulmenţi. Standul este folosit pentru diagnoza vibroacustică a defectelor organelor de maşini componente. Ordinele măsurate experimental sunt asociate vibraţiilor generate în funcţionarea normală a standului şi pentru anumite defecte inerent existente din construcţie. Se urmăreşte în continuare detectarea si clasificarea unor defecte folosind tehnici de învăţare automată folosind inteligenţa artificială.

Iulian LUPEA, Professor Ph.D., Technical University of Cluj-Napoca, Department of Mechanical Systems Engineering, 103-105 Muncii Blvd., 400641 Cluj-Napoca, ☎+40-264-401691, e-mail: iulian.lupea@mep.utcluj.ro ; www.viaclab.utcluj.ro